

The Spinning Cyclic ‘Miura-oRing’ for Mechanical Collision-Resilience

Pooya Sareh, Pisak Chermprayong, Marc Emmanuelli,

Haris Nadeem, and Mirko Kovac

Abstract: *Impact protection structures enable aerial robots to navigate in confined or cluttered environments. As weight is a major limitation in designing aerial vehicles, origami-inspired folded structures made of thin material sheets can offer novel, lightweight solutions to tackle collision resilience challenges. Here, we study the use of energy absorption properties of origami structures for the protection of a miniature aerial robot in horizontal collisions. A ring-shaped, cyclic symmetric descendant of the Miura-ori, which we call the ‘Miura-oRing’ in this paper, is studied. It acts as a light-weight radial spring used as a collision-cushioning structure to be assembled on a quadrotor frame in order to provide horizontal impact protection.*

1 Introduction

Effective structural impact protection is a major consideration in the design of both manually-driven and autonomous vehicles in all modes of transport. On the other hand, energy consumption is a significant factor limiting the structural mass of vehicles. This constraint becomes more significant for aerial vehicles, as the propulsion system needs to generate enough lift to take the vehicle off the ground. As a result, designing high-performance, lightweight protective structures is an important challenge in the development of collision-resilient and energy-efficient vehicles in all terrains.

Thin-walled structures have been used as energy absorption devices in vehicle design as a result of their favourable structural characteristics such as high strength-to-weight ratio. A well-known example is the crash box in automobiles, a thin-walled member attached to the front rail and bumper of the vehicle for energy absorption in collisions. Similar thin-walled elements are used in the structural design of trains to minimise damage and fatalities in case of an accident [Marsolek and Reimerdes 04].

1.1 Structural behaviour of origami structures

Origami folded sheets can be generally considered to be thin-walled structures. This has paved the way for the development of novel thin-walled structures with desirable properties based on the rich literature of origami design. Many researchers have studied the structural behaviour of various origami-inspired thin-walled structures under different mechanical loadings, of which several examples are represented in Figure 1.

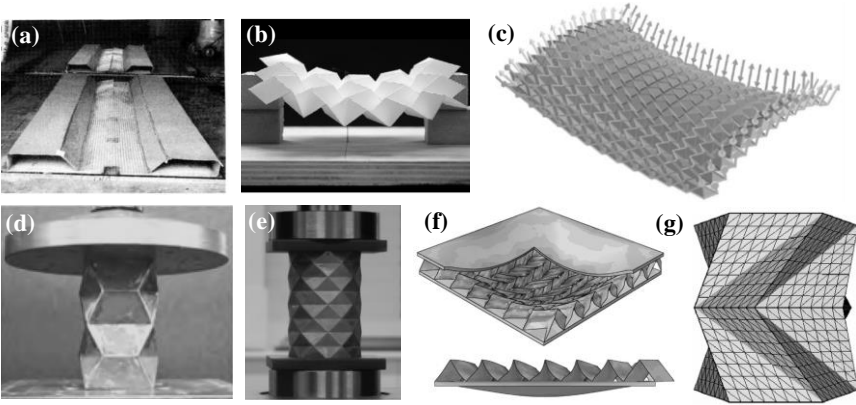


Figure 1: Examples of studies on the structural behaviour of various origami structures. (a) Concrete origami building panels tested for performance under transverse loads [Holland and Jones 84]. (b) Three-point bending experiment of a Miura-ori paper model [Schenk 11]. (c) Numerical simulation of the bending response of a Miura-ori plate [Wei et al. 13]. (d & e) Axial crushing test of different origami tubes [Ma and You 14 & Yang 18]. (f) Deformed shape of the Miura-ori core sandwich plate under a blast load [Pydah and Batra 17]. (g) Optimisation of the crush characteristics of a cylindrical origami structure with triangular facets [Wu et al. 07].

1.2 Origami-inspired vehicular robotics

Over the past few decades, origami design principles have found numerous innovative applications in various branches of engineering. In recent years, robotics has been a fast-growing field of application for origami engineering. In particular, origami-inspired structures have played substantial roles in the design of novel reconfigurable robotic vehicles such as the self-folding crawling robot. A number of examples for such applications of origami are depicted in Figure 2.

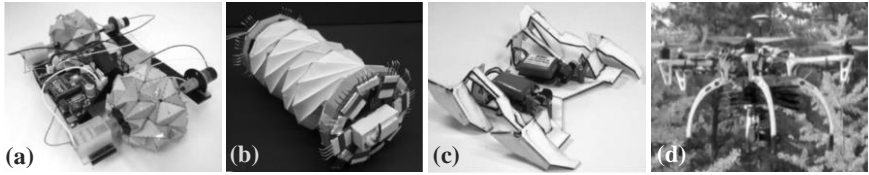


Figure 2: *Examples for the applications of origami-inspired reconfigurable structures in vehicular robotics. (a) Deformable wheel robot using the magic ball origami [Lee et al. 13]. (b) Multi-stable crawling robot [Pagano et al. 16]. (c) Self-folding crawling robot [Felton et al. 14]. (d) Self-locking foldable robotic arm [Kim et al. 18].*

In this paper, we aim to demonstrate the application of the favourable structural properties of a derivative of a well-known origami pattern in the development of a collision-resilient aerial robot.

2 Origami-inspired Mechanical Collision-Resilience: A Case Study on Aerial Robots

As discussed in the previous section, a diverse range of successful applications of origami in robotics have been demonstrated by the research community. However, most of these applications have been developed based upon the reconfigurability properties of origami structures through geometric transformations. In fact, other potentially useful aspects of origami structures such as energy absorption properties have not attracted much attention in robotic design. Here, we aim to demonstrate the utility of lightweight energy-absorbent origami structures in vehicular robotics through a case study on collision-resilient aerial robots.

Flying robots, or drones, are rapidly becoming a part of our everyday lives. Currently, collision-resilience and safety are among the most important challenges on the way of wide-spread commercialisation of multirotor drones. Remote sensing is a widely-used strategy to avoid potential collisions [Modi et al. 01, Merrell et al. 04, Kwag and Chang 07, Odelga et al. 16]. However, most remote sensors are not capable of detecting all possible impact scenarios. Furthermore, they significantly add to the computational complexity of the vehicle's onboard equipment.

A collision robust flying robot – resilient to physical impact with obstacles – is highly useful for flight operations in confined or cluttered environments. Commercially available mechanical protection concepts are not sufficiently effective, and are often based on rigid components that do not mitigate collision forces. For example, propeller guards made of Expanded/Extruded Polystyrene foam (EPS/XPS) are used as a light-weight and inexpensive solution for the protection of commercial multirotor drones. However, as EPS and XPS are both

rigid materials with poor elastic behaviour [Gibson and Ashby 99, Mcvicker, 17], they are unable to properly cushion impact forces in a recoverable manner.

Inspired by the energy absorption capacities and lightweight of folded polymer sheets, in this paper we propose an origami-inspired protective structure for miniature flying robots (see Fig. 3a for an artist impression).

3 The Cyclic ‘Miura-oRing’: Design and Simulation

It has been shown that the most effective protective configuration against horizontal collisions is a decoupled (i.e. passively spinning) universal (i.e. protecting all propellers) protector [Kovac and Sareh 18]. Theoretically, assuming the centre of the universal protector is coincident with the centre of mass of the aerial vehicle, and the friction in rotational joints between the platform and the protector is negligible, a decoupled universal protector will eliminate all yawing moments arising due to the collision.

In addition to moment decoupling as a first strategy, a second strategy to enhance the impact-robustness of aerial robots is to minimise the peak collision force experienced by the platform. Here we study the functionality of an origami impact protector made of a very thin plastic sheet.

The Miura-ori [Miura 85] (Fig. 3b) is a widely-used origami tessellation in engineering design. Several studies have proposed symmetric derivatives for this pattern which can alter both the form and functionality of the original pattern (see, e.g. [Klett and Drechsler 10]). Variations with finite symmetry groups include several descendants with rosette symmetry (i.e. two-dimensional point groups) including cyclic and dihedral descendants. Using a group-theoretic framework, an extensive family of isomorphic [Sareh and Guest 13, 14, 15a] and non-isomorphic [Sareh and Guest 12 & 15b] wallpaper [Hahn 05] symmetric variations for this pattern have been designed. Based on a cyclic variation of the Miura-ori [Barreto 97, Nojima 02], we aim to develop a protector capable of reducing the peak force experienced by the vehicle in a collision. In this paper, we call this variation the cyclic ‘Miura-oRing’.

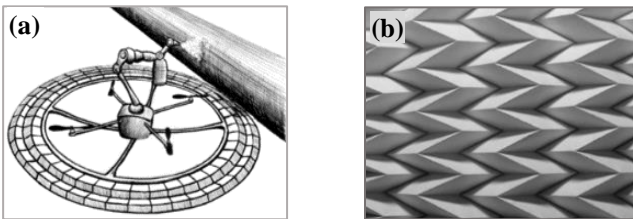


Figure 3: (a) Artist’s impression of a quadrotor equipped with an origami bumper for safe and crash-robust pipe inspection and repair. (b) The Miura-ori in a partially folded state [Sareh, 2014].

3.1 Geometric Modelling of the Cyclic Miura-oRing

Modelling the cyclic Miura-oRing as a function of five geometric parameters enabled us to produce an array of different models which served as inputs to finite element analysis (FEA). The five parameters which fully define the cyclic origami pattern (Fig. 4) are:

i. Number of radial segments (n): This is the number of segments into which the circle is divided, depicted as $S_1, S_2, S_3, \dots, S_n$ in Fig. 4. It has to be an even number to keep the number of mountain and valley fold lines equal. In this model, it ranges from 30° to 70° .

ii. Pattern angle (α): Changing one angle will affect all others as there is only one degree of freedom dictating all angles in this origami pattern. In this model, we decided to change the acute angle of the most internal facets from 20° to 50° .

iii. Inner diameter (r): The inner diameter shrinks as the origami ring is folded. An empirical function was established from folding. We estimated the suitable inner diameter of the two-dimensional pattern in order for the folded structure to fit around the circular protective frame of the drone.

iv. Number of concentric layers (m): This is the number of layers in the radial direction, depicted as $l_1, l_2, l_3, \dots, l_m$ in Fig. 4. For simplicity and to focus on continuous parameters, this value was held constant at 5 in our model, and we did not investigate the effects of varying this parameter on structural performance.

v. Width of external facets (w_e): The width of facets on the external edge of the pattern provides an extra degree of freedom. This parameter, w_e , is expressed as a factor of the unchanged facet width w_u , i.e., $\dot{w} = w_e/w_u$, where w_e is the external facet width and w_u is the unchanged facet width in the pattern sequence. In this study, the normalised width \dot{w} was set to range from 0.6 to 1.4.

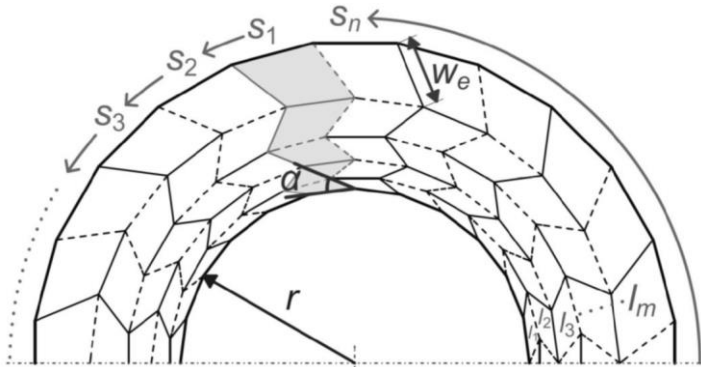


Figure 4: Geometric modelling of the cyclic Miura-oRing: Half of a typical crease pattern and its geometric parameters (mountain and valley folds are represented by solid and dashed lines, respectively).

3.2 Finite Element Analysis

The two parameters which affect the overall geometry of the structure are the number of radial segments n , and the pattern angle α , which composed a set of models to be simulated (Fig. 5). The origami ring was a thin-walled structure, and the miniature drone was a low-speed, light-weight vehicle. As a result, in order to choose a suitable design for the ring, we adapted the quasi-static FEA simulation method which is widely used for the evaluation of impacts of thin-walled structures [Mamalis and Johnson 83, Zheng et al. 04, Ma and You 14]. The simulations involved displacing a rigid plate towards the centre of the origami structures. By performing a series of identical simulations on origami structures with varying geometric parameters, it was possible to carry out a comparative analysis, relating those parameters to the stiffness and energy absorption capabilities of the structures under compression. The origami structures were meshed using S4R shell elements in Abaqus/Explicit (S4R is a general purpose, doubly-curved, linear four-sided shell element). The formulation of the element allows for six degrees-of-freedom per node. The model was meshed using an approximate element size of 1.7 mm. After processing the FEA results, the structural behaviour of each model was determined (Fig. 6). Specific outputs were extracted from the resulting force vs. displacement curves to characterise the structural performance of each model for the purpose of choosing a suitable design. These outputs were: (i) the elastic energy (temporarily) absorbed by the structure until it slips out of plane, (ii) the peak reaction force during compression, and (iii) the mass of the structure. It is desirable to have a lightweight protective structure with high elastic energy absorption capacity, i.e. a structure with high specific elastic energy (elastic energy per unit mass). Furthermore, in order to minimise the risk of damage to the vehicle, the protective ring must have a relatively low peak reaction force during compression.

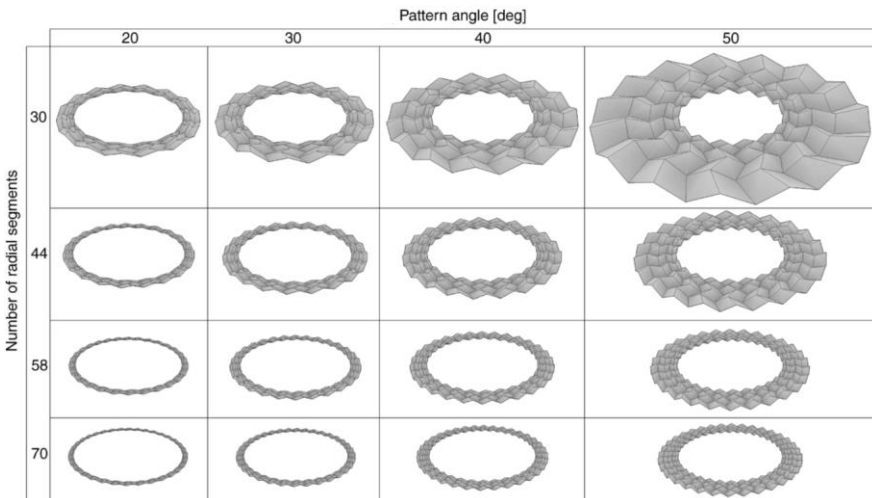


Figure 5: Matrix of models tested for parameters α and n whilst $w=1$.

The specific energy analysis indicated that, in general, a more desirable design can be achieved by choosing a pattern angle of 30° (see Fig. 7). Also, it was observed that, as a general trend, increasing the number of radial segments increases the peak reaction force.

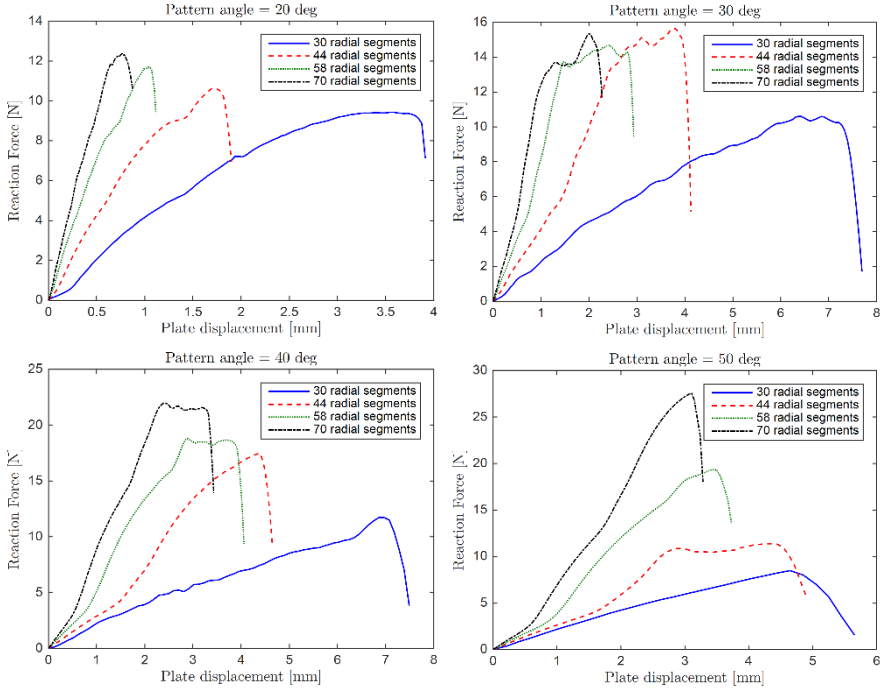


Figure 6: Finite element analysis output data from simulations of the matrix of models in the previous figure.

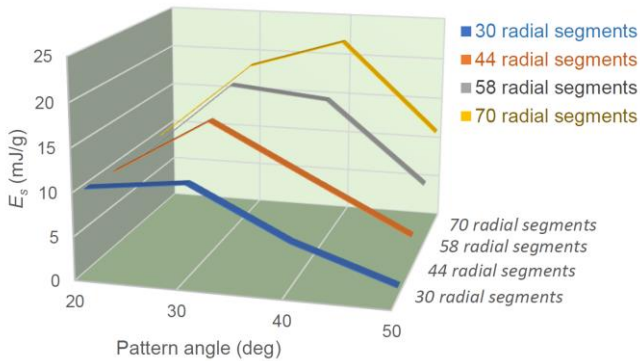


Figure 7: Specific energy (E_s) for the Miura-oRing models with different pattern angles and number of radial segments.

4 Fabrication, Experimentation, and Results

In addition to the structural design considerations, and in order to provide a well-suited design for the intended application, we took into account the manufacturability of the structure at small scale (to suit the palm-sized flying robot used in this study) as an extra design consideration. In fact, whilst increasing n at a constant α would create a more desirable ring in terms of structural performance, it also makes the hand-folding process increasingly difficult. This is due to two reasons. Firstly, increasing n proportionally increases the number of internal vertices of the structure. This not only increases the number of lines to be folded, but makes the facets progressively smaller. Keeping in mind the limits of manual fabrication, as the facets become smaller, folding the pattern without damage to internal facets poses a substantial fabrication challenge. As a result, for the given size of the ring, we manufactured a structure with $n = 40$ as a reasonable trade-off between structural performance and manufacturability.

To verify the capabilities of the proposed protective concept, impact experiments were carried out with a miniature multirotor aerial robot (Crazyflie 2.0) as depicted in Fig. 8. The following are the four design configurations which were tested for their impact resilience performance: C₁: fixed naked, C₂: rotary naked, C₃: fixed origami-protected, and C₄: rotary origami-protected shields. The peak impact force and angular speed of these design configurations were measured and analysed to compare their corresponding impact protection performances in normal and oblique collisions. In these experiments, pendulum swing tests were performed using the quadcopter, equipped with an inertial measurement unit (IMU), as a pendulum mass.

To obtain certain collision velocities, a simple energy conservation equation between potential and kinetic energy ($E = mgh = 0.5mv^2$) has been used to calculate the required height at a pendulum releasing point, where E is the total amount of mechanical energy, m is the pendulum mass, h is the height of the pendulum from the releasing point to the point of impact, and v is the velocity upon impact to the wall. An electromagnet was used to hold and release the vehicle precisely to make sure that each collision has the same initial velocity and initial orientation for each testing configuration. A maximum velocity of 1.2 m/s at the lowest point of the pendulum swing was set as a typical target velocity to simulate a horizontal collision to a surface. It should be mentioned that the masses of the naked and origami protector were not the same due to the added weight of the origami structure; the origami protected configurations had a mass of 53.0 g, while the naked configurations were both 48.5 g. Hence, the impact forces were calculated from the actual mass of each design configuration. The impact surfaces were switched between smooth (acrylic glass) and rough (sandpaper with ISO Grit P80) in order to determine the effect of the friction coefficient of hitting surfaces. The swing of the pendulum was oriented at two different angles to simulate impacts at two different angles of collision with respect to the colliding surface: 30° (oblique

collision) and 90° (normal collision). For each collision scenario, we calculated the average values of force and angular speed from five trials.

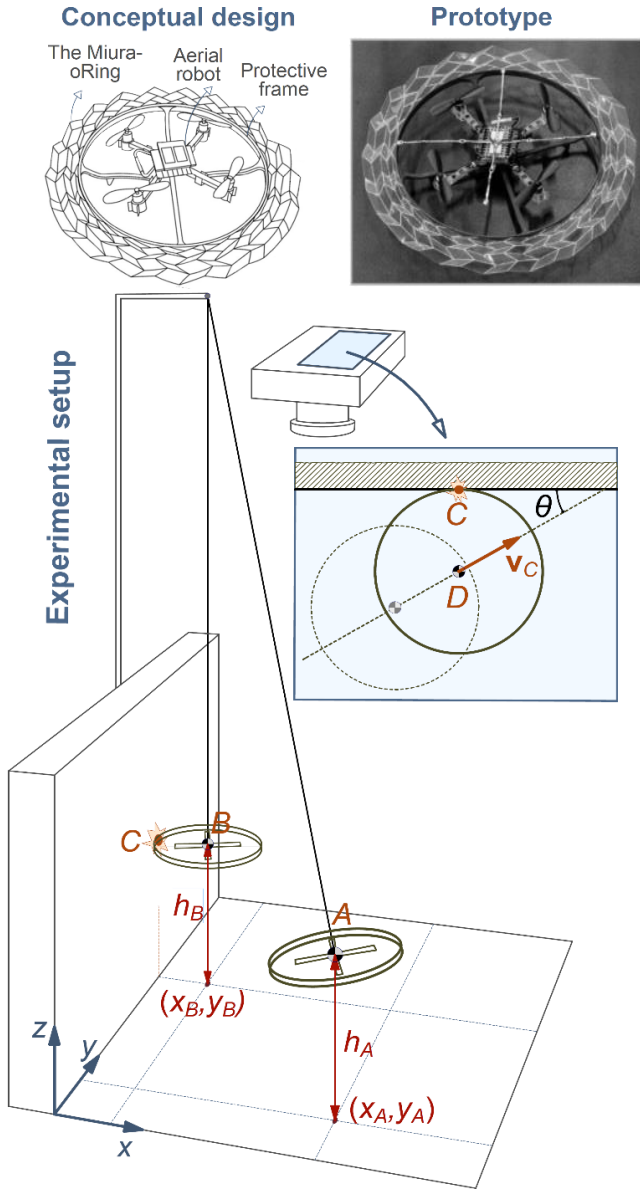


Figure 8: Top: Conceptual design and prototype for a palm-sized quadrotor drone with a spinning Miura-oRing protector. Bottom: Schematic experimental setup for the pendulum collision tests of the quadrotor to a surface.

The collision duration in the origami-protected systems was observed to be significantly longer than that of the naked systems, providing a considerable level of impact cushioning. We began by comparing the impact protection performance between the naked and origami-protected systems in a normal collision. At this collision angle (i.e. 90°), the peak force reduction turned out to be around 30% for both fixed and rotary origami-protected systems when compared to the naked configurations. For impacts at 30° with respect to the collision surface, in which the tangential collision force is dominant, the peak force reduction was around 20%.

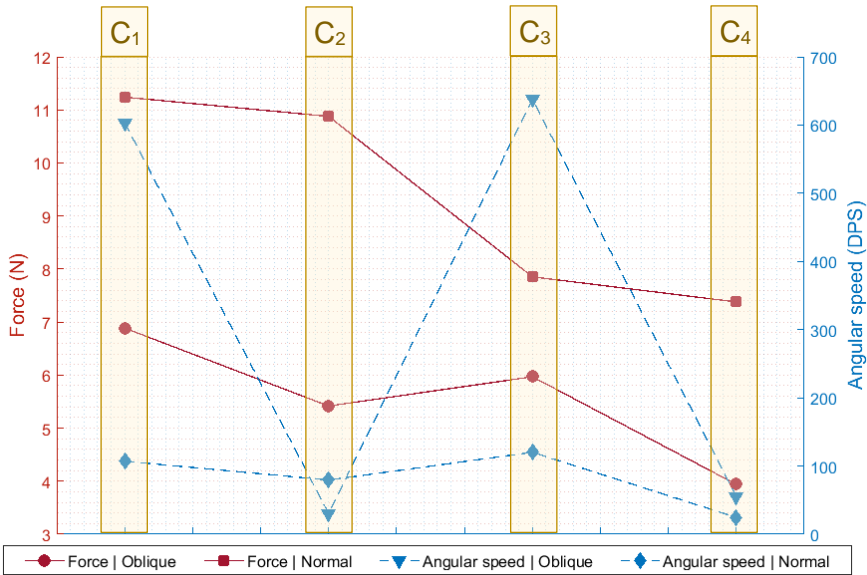


Figure 9: Summary of experimental results for four design configurations: C₁: fixed naked, C₂: rotary naked, C₃: fixed origami-protected, and C₄: rotary origami-protected. Values have been averaged between the results of experiments using rough and smooth surfaces.

In order to investigate the performance of the rotary configurations compared to the fixed ones, force and angular speed data were analysed in a way similar to the previous section. The effect of the rotary concept on the reduction of rotational speed after impact was clearly demonstrated in the 30° impact experiments where the tangential component of collision force was relatively large. As anticipated, every fixed protection system displayed considerably higher rotational speed after impact compared to the rotary systems. Specifically, the fixed protection systems were not effective against the rough surface in sliding collisions as the average maximum angular speed for fixed naked and fixed origami-protected systems were

recorded to be around 814 and 697 degrees per second (DPS), respectively. Even though those values for the fixed protection system on the smooth surface were lower compared to those of the rough surface due to lower friction, they were still significantly high: around 392 and 579 DPS for the fixed naked and fixed origami-protected systems, respectively. On the contrary, the rotary systems effectively decoupled shear impact force, resulting in an average maximum angular speed of one order of magnitude smaller compared to those of the fixed protection systems in the collision scenarios above. In normal collisions, the fixed and rotary systems performed similarly as expected due to the dominance of the normal component of the collision force. The experimental results are summarised in Fig. 9.

5 Conclusions

We developed and demonstrated an effective protection system that can cushion the impact to reduce the overall collision peak force experienced by the drone, as well as decouple the induced yawing moment from the platform. Studies on both smooth and rough surfaces demonstrated that the simultaneous exploitation of these two concepts is the most advantageous design configuration in terms of the overall impact protection performance. In summary, origami-protected systems offered 20~30% improvement in the peak impact force reduction compared to naked-protection systems in all tested collision scenarios.

References

- [Barreto 97] Paulo Taborda Barreto. "Lines Meeting on a Surface: The 'Mars' Paperfolding." In *Origami Science & Art: Proceedings of the Second International Meeting of Origami Science and Scientific Origami*, Otsu, Japan, 1997, pp. 343-359.
- [Felton et al. 14] S. Felton, M. Tolley, E. Demaine, D. Rus, and R. Wood. "A method for building self-folding machines." *Science* 345 (6197), 644-646.
- [Gibson and Ashby 99] Lorna J. Gibson and Michael F. Ashby. *Cellular Solids: Structure and Properties* (Cambridge Solid State Science Series), Cambridge University Press, 1999.
- [Hahn 05] T. Hahn. *International Tables for Crystallography* (Volume A: Space-group symmetry), Springer, USA, 2005.
- [Holland and Jones 84] Graham E. Holland and Meredith Trevallyn-Jones. "The Structural Behaviour of Concrete Origami Building Panels." *Architectural Science Review*, 1984.
- [Kim et al. 18] Suk-Jun Kim, Dae-Young Lee, Gwang-Pil Jung, and Kyu-Jin Cho. "An origami-inspired, self-locking robotic arm that can be folded flat." *Sci. Robot.* 3, eaar2915 (2018).
- [Klett and Drechsler 10] Yves Klett and Klaus Drechsler. "Designing Technical Tessellations." *5th International Meeting on Origami in Science, Mathematics and Education* (5OSME), Singapore, 2010.

- [Kovac and Sareh 18] Mirko Kovac and Pooya Sareh. "Aerial Devices Capable of Controlled Flight.", United States Patent Application 2018/0155018 A1. Assignee: Imperial Innovations Limited, UK; filing date: 05/27/2016; publication date: 06/07/2018; Available at: <http://www.freepatentsonline.com/20180155018.pdf>.
- [Kwag and Chang 07] Young K. Kwag and Chul H. Chung. "UAV based collision avoidance radar sensor." IEEE International Geoscience and Remote Sensing Symposium, Barcelona, Spain, 2007.
- [Lee et al. 13] D. Lee, J. Kim, S. Kim, J. Koh, K. Cho. "The Deformable Wheel Robot Using Magic-Ball Origami Structure." ASME International Design Engineering Technical Conferences and Computers and Information in Engineering Conference, Volume 6B: 37th Mechanisms and Robotics DETC2013.
- [Ma and You 14] Jiayao Ma and Zhong You. "Energy Absorption of Thin-Walled Square Tubes With a Prefolded Origami Pattern - Part I: Geometry and Numerical Simulation." Journal of Applied Mechanics. 2014. - 1 : Vol. 81.
- [Mamalis and Johnson 83] A.G. Mamalis and W. Johnson. "The quasi-static crumpling of thin-walled circular cylinders and frusta under axial compression." International Journal of Mechanical Sciences. - 1983. - 9-10 : Vol. 25. - pp. 713-732.
- [Marsolek and Reimerdes 04] J. Marsolek and H.G. Reimerdes. "Energy absorption of metallic cylindrical shells with induced non-axisymmetric folding patterns." International Journal of Impact Engineering, Vol. 30, 2004.
- [McVicker 17] S. McVicker. "Shear Wall Basics." McVicker Associates, Inc., 2017. Available at: <http://www.mcvicker.com/vwall/page003.htm>
- [Merrell et al. 04] P.C. Merrell, D. Lee, and R. W. Beard. "Obstacle avoidance for unmanned air vehicles using optical flow probability distributions." Proc. SPIE 5609, Mobile Robots XVII, 2004.
- [Miura 85] Koryo Miura. "Method of Packaging and Deployment of Large Membranes in Space." The Institute of Space and Astronautical Science Report, 1985,618, pp. 1-9.
- [Modi et al. 01] Sachin Modi, Pravin Chandak, Vidya Sagar Murty, and Ernest L. Hall. "A Comparison of Three Obstacle Avoidance Methods for a Mobile Robot." Proceedings of SPIE, 2001.
- [Nojima 02] Taketoshi Nojima. "Modelling of Folding Patterns in Flat Membranes and Cylinders by Origami." JSME International Journal Series C, 2002. 1 : Vol. 4, pp. 364-370.
- [Odelga et al. 16] Marcin Odelga, Paolo Stegagno, and Heinrich H. Bühlhoff. "Obstacle Detection, Tracking and Avoidance for a Teleoperated UAV." IEEE International Conference on Robotics and Automation (ICRA), Stockholm, Sweden, 2016.
- [Pagano et al. 16] A. Pagano, B. Leung, B. Chien, T. Yan, A. Wissa and S. Tawfick. "Multi-Stable Origami Structure for Crawling Locomotion." ASME Smart Materials, Adaptive Structures and Intelligent Systems, Vol. 2: Modeling, Simulation and Control; Bio-Inspired Smart Materials and Systems; Energy Harvesting SMASIS2016-9071.

- [Pydah and Batra 17] A. Pydah and R.C. Batra. "Crush dynamics and transient deformations of elastic-plastic Miura-ori core sandwich plates." *Thin-Walled Structures*, 2017, Vol. 115, pp 311-322.
- [Sareh and Guest 12] Pooya Sareh and Simon D Guest. "Tessellating Variations on the Miura Fold Pattern." IASS-APCS Symposium, Seoul, South Korea 2012.
- [Sareh and Guest 13] Pooya Sareh and Simon D Guest. "Minimal Isomorphic Symmetric Variations on the Miura Fold Pattern." *First International Conference Transformables-2013*, Seville, Spain, 2013.
- [Sareh and Guest 14] Pooya Sareh and Simon D Guest. "Designing Symmetric Derivatives of the Miura-ori." *Advances in Architectural Geometry*, 2014, London, UK,.
- [Sareh 14] Pooya Sareh. "Symmetric Descendants of the Miura-ori." PhD Dissertation, Engineering Department, University of Cambridge, UK, 2014.
- [Sareh and Guest 15a] Pooya Sareh and Simon D Guest. "A Framework for the Symmetric Generalisation of the Miura-ori." *International Journal of Space Structures*, Vol. 30 No. 2, 2015.
- [Sareh and Guest 15b] Pooya Sareh and Simon D Guest. "Design of non-isomorphic symmetric descendants of the Miura-ori." *Smart Materials and Structures*, 2015, Vol. 24, No. 8, pp. 13-28 (085002).
- [Schenk 11] Mark Schenk. "Folded Shell Structures." PhD Dissertation, Engineering Department, University of Cambridge, UK, 2011.
- [Wei et al. 13] Z. Y. Wei, Z. V. Guo, L. Dudte, H. Y. Liang, L. Mahadevan. "Geometric Mechanics of Periodic Pleated Origami." *Phys. Rev. Lett.* 110, 215501 – 2013.
- [Wu et al. 07] Z. Wu, I. Hagiwara, and X. Tao. "Optimisation of crush characteristics of the cylindrical origami structure." *Int. J. Vehicle Design*, Vol. 43, Nos. 1-4, 2007.
- [Yang 18] Kai Yang. "Design Optimization of Energy Absorption Structures with Origami Patterns." PhD Thesis, School of Engineering, RMIT University, Australia, 2018.
- [Zheng et al. 04] L. Zheng and T. Wierzbicki. "Quasi-static crushing of S-shaped aluminum front rail." *International Journal of Crashworthiness*, 2 : Vol. 9. 2004 - pp. 155-173.

Pooya Sareh

Division of Industrial Design, School of Engineering, University of Liverpool,
London Campus, London, EC2A 1AG, UK, & Aerial Robotics Lab, Aeronautics
Department, Imperial College London, South Kensington, London, SW7 2AZ, UK
e-mail: pooya.sareh@liverpool.ac.uk

Pisak Chermprayong

Aerial Robotics Lab, Aeronautics Department, Imperial College London, South
Kensington, London, SW7 2AZ, UK
e-mail: pisak.chermprayong10@imperial.ac.uk

Marc Emmanuelli

Aerial Robotics Lab, Aeronautics Department, Imperial College London, South
Kensington, London, SW7 2AZ, UK
e-mail: emmanuellimarc@gmail.com

Haris Nadeem

Aerial Robotics Lab, Aeronautics Department, Imperial College London, South
Kensington, London, SW7 2AZ, UK
e-mail: haris.nadeem15@imperial.ac.uk

Mirko Kovac

Aerial Robotics Lab, Aeronautics Department, Imperial College London, South
Kensington, London, SW7 2AZ, UK
e-mail: m.kovac@imperial.ac.uk